Available online at www.sciencedirect.com

ScienceDirect

Nuclear Instruments and Methods in Physics Research B 266 (2008) 791–796

NIM B
Beam Interactions with Materials & Atoms

www.elsevier.com/locate/nimb

Effects of γ-ray irradiation on the C–V and G/ω–V characteristics of Al/SiO_2/p-Si (MIS) structures

İlbilge Dökme [a,*], Perihan Durmuş [b], Şemsettin Altındal [b]

[a] Science Education Department, Faculty of Education, Ahi Evran University, Kırşehir, Turkey
[b] Physics Department, Faculty of Arts and Sciences, Gazi University, 06500 Teknikokullar, Ankara, Turkey

Received 5 June 2007; received in revised form 7 January 2008
Available online 20 January 2008

Abstract

The effect of the $^{60}C_o$ (γ-ray) exposure on the electrical characteristics of Al/SiO_2/p-Si (MIS) structures has been investigated using capacitance–voltage (C–V) and conductance–voltage (G/ω–V) measurements. The MIS structures were stressed with a bias of 0 V during $^{60}C_o$ γ-sources irradiation with the total dose range from 0 to 25 kGy. The C–V and G/ω–V characteristics were measured at 500 kHz and room temperature before and after $^{60}C_o$ γ-ray irradiation. The results indicated that γ-irradiation caused an increase in the barrier height Φ_B, interface states N_{ss} and depletion layer width W_D obtained from reverse bias C–V measurements. The series resistance R_s profile for various radiation doses was obtained from forward and reverse bias C–V and G/ω–V measurements. Both C–V and G/ω–V characteristics indicate that the total dose radiation hardness of MIS structures may be limited by the decisive properties of the SiO_2/Si interface to radiation-induced damage. After γ-irradiation, the decrease in capacitance of MIS structure results in the increase in the semiconductor depletion width.

PACS: 61.80.−x; 73.40.Qv; 84.37.+q; 73.20.−r

Keywords: γ-ray effects; Schottky diodes; C–V and G/ω–V characteristics; Series resistance; Interface states

1. Introduction

The existence of an insulator layer between metal and semiconductor convert the metal–semiconductor (MS) diodes into MIS diodes. The electrical characteristics of these devices are extremely sensitive to interface states density at semiconductor/insulator interface. When the ionizing particles (gamma, electrons, protons, ions, etc.) expose on these diodes, they may cause strong electrical changes in MIS structures [1–12]. Especially, there are two important effects to be considered: (a) the transient effects due to electron–hole pair generation and (b) permanent effect due to radiation damage, causing change in the crystal lattice. The radiation-induced defects act as recombination centers trapping the generated carriers, degrading the diode performance and applications. The radiation-generated electrons either recombine with the holes or move out of the insulator. The radiation-generated holes may diffuse in the insulator, but are less mobility than the electrons; many stationary holes traps are also present.

Although there are many studies on the effect of radiation on MS, MIS or MOS devices [1–11], after-irradiation behavior of electrical characteristics of such devices have not been fully reported. Ma [1,10] and Winokur et al. [8,9] were among the first to make a systematic observation of the after-irradiation behavior of radiation-induced interface traps in MIS and MOS devices. Interface traps, also known as interface states or surface states, are electronic energy levels located at the Si/SiO_2 interface and are important parameters like series resistance.

---

[*] Corresponding author.
E-mail address: ilbilgedokme@gazi.edu.tr (İ. Dökme).

doi:10.1016/j.nimb.2008.01.017

In this work, we present results of a study on the effect of γ-ray irradiation on the electrical characteristics of Al/SiO_2/p-Si Schottky diodes. We exposed a maximum cumulative dose of 25 kGy on the diode at room temperature. After each radiation dose, we report on the changes in electrical characteristics evaluated using forward and reverse bias C–V and G/ω–V measurements. We also report on the bias dependence of the R_s profile for various radiation doses.

2. Experimental detail

The Al/SiO_2/p-Si (MIS) structures used in this study were fabricated using p-type (boron-doped) single crystals silicon wafer with $\langle 111 \rangle$ surface orientation having thickness of 300 μm, 5.08 cm diameter and 4 Ω cm resistivity. For the fabrication process, Si wafer was degreased in organic solvent of $CHClCCl_2$, CH_3COCH_3 and CH_3OH consecutively and then etched in a sequence of H_2SO_4 an H_2O_2, 20% HF, a solution of $6HNO_3$:1 HF:$35H_2O$, 20% HF and finally quenched in de-ionized water for a prolonged time. Preceding each cleaning step, the wafer was rinsed thoroughly in de-ionized water of resistivity of 18 M Ω cm. Immediately after surface cleaning, to form ohmic contacts on the back surface of the Si wafer, high purity aluminum (Al) metal (99.999%) with a thickness of ~2000 Å was thermally evaporated from the tungsten filament onto the whole back surface of the Si wafer in the pressure of $\sim 2 \times 10^{-6}$ Torr in vacuum pump system and the evaporated Al was sintered. The oxidation process is carried out in a resistance-heated furnace in dry oxygen with a flow rate of a 1.5 l/min and the oxide layer is grown at the temperature of 900 °C during 2 h. To form the Schottky contacts, the circular dots of ~2 mm diameter and ~2000 Å thick Al are deposited onto the oxidized surface of the wafer for through a metal shadow mask in a liquid nitrogen trapped vacuum system at the pressure of $\sim 2 \times 10^{-6}$ Torr. The interfacial oxide layer thickness was estimated to be about 36 Å from high frequency (500 kHz) measurement of the interface oxide capacitance in the strong accumulation region for MIS Schottky diode [13].

The capacitance–voltage (C–V) and conductance–voltage (G/ω–V) measurements were carried out using an HP 4192 A LF impedance analyzer (5 Hz–13 MHz). A low-distortion oscillator generated the ac signal with the amplitude attenuated to 50 mV_{rms} to meet the small signal requirement for oxide capacitors [13]. The C–V and G/ω–V measurements were performed before and after ^{60}Co γ-ray source irradiation with the dose rate of 2.12 kGy/h and total dose range was 0–25 kGy at 500 kHz under dark condition at room temperature. Irradiation dose is referred to the water in Gamma cell at Sarayköy Nuclear Research and Training Center in Ankara, Turkey. All measurements were carried out with the help of a microcomputer through an IEEE-488 ac/dc converter card.

3. Results and discussion

The depletion layer capacitance in MIS and MOS structures can be expressed as [13–15]

$$C^{-2} = \frac{2(V_o + V)}{\varepsilon_s \varepsilon_o q A^2 N_A}, \tag{1}$$

$$\frac{d(C^{-2})}{dV} = \frac{2}{\varepsilon_s \varepsilon_o q A^2 N_A}, \tag{2}$$

where A is the area of diode, ε_s is the dielectric constant of semiconductor ($11.8\varepsilon_0$ for Si), ε_o is the dielectric constant of vacuum (8.85×10^{-14} F/cm), N_A is the acceptor concentration of p-type Si, q is the electronic charge, V is the applied reverse bias and V_o is the intercept of C^{-2} versus V plot with the voltage axis and is given by

$$V_o = V_D - kT/q, \tag{3}$$

where V_D is the diffusion potential, T is the absolute temperature in K and k is the Boltzmann constant.

The value of the barrier height (Φ_B) can be obtained from the reverse bias C–V characteristics by the relation

$$\Phi_B = V_D + E_F - \Delta\Phi_B = V_D + \left(\frac{kT}{q}\right) \ln\left(\frac{N_V}{N_A}\right) - \Delta\Phi_B, \tag{4}$$

where E_F is the energy difference between the bulk Fermi level and valance band edge, N_V is the effective density of states in valance band and $\Delta\Phi_B$ is the image force barrier lowering and can be obtained from the well-known relationship in [13–19].

It is well-known that in the low frequencies N_{ss} can easily follow the ac signal and yield an excess capacitance, which depends on the frequency, but in the high frequency limit ($f \geqslant 500$ kHz), the interface states cannot follow the ac signal. This makes the contribution of interface state capacitance to the total capacitance negligibly small [20,21]. Also, the C–V and G/ω–V measurements at high frequency (≅500 kHz) are relatively easily and rapidly carried out and these measurements can yield interesting and meaningful results to show the negligibility of excess capacitance. Therefore, the C–V and G/ω–V characteristics were measured at sufficiently high frequency (500 kHz).

Fig. 1 shows a typical C–V relation obtained from the measurement at high frequency of 500 kHz and room temperature before and after γ-ray irradiation, which manifests the presence of the trapping centers [12,16–19]. It is clear that for p-type substrate, electrons accumulate underneath SiO_2 at negative gate bias. A shift of the C–V data from inversion toward the accumulation region decreases with the increase in radiation dose. By analyzing the high frequency curves in Fig. 1, it is clearly seen the decreasing values of the capacitance with increasing radiation dose and the stretch-out of the C–V curves under the influence of irradiation, reflecting the generation of oxide charge due to electron–hole pair generation by the radiation [1,6,19]. The decrease in C with increase in dose especially at reverse

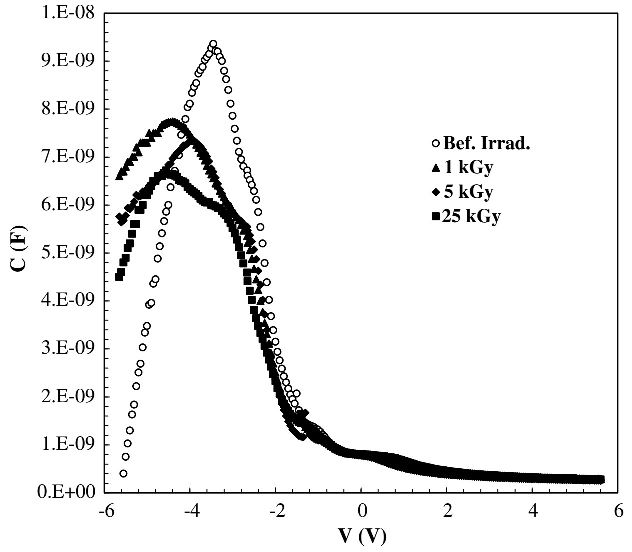

Fig. 1. The C–V characteristics of the Al/SiO$_2$/p-Si Schottky diode before and after γ-ray irradiation at 500 kHz and room temperature.

bias results in the increase in the semiconductor depletion width.

The C–V curves give peaks in the depletion region due to the particular distribution of interface states between SiO$_2$/Si interface and effect of series resistance, respectively. The magnitude of the peaks is decreased with increasing irradiation dose. This behavior may be understood in terms of the radiation-induced N_{ss} as shown in Table 1 and the space–charge which consisted of mobile ions generated by irradiation in oxide. Depending on the relaxation time of the density of interface states (N_{ss}) and the frequency of the ac signal, there may be a capacitance due to interface states in excess to depletion layer capacitance.

Fig. 2 shows the reciprocal of the squared capacitance as a function of the bias before and after γ-ray irradiation between 0 and 25 kGy. As can be seen in Fig. 2, the C^{-2}–V variation is linear in the wide voltage range of 0.85–2 V at sufficiently high frequency (such that carrier life time τ is much larger than $1/2\pi f$) [14]. This linearity of the curve is attributed to the uniformity of the N_A in the depletion region, indicating the interface states cannot follow ac signal at high frequencies. The relationship of the theoretical carrier doping density N'_A and the experimental carrier doping density N_A is known as $c_2 \cong N_A/N'_A$. Thus, the mean density of interface states N_{ss} were calculated from C to V characteristics at 500 kHz frequency for different radiation doses by using the equation [20–25]

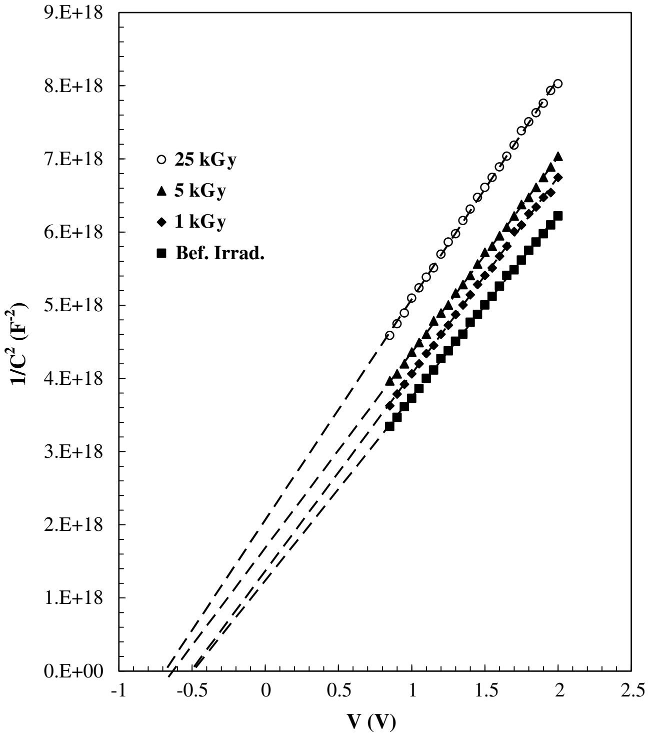

Fig. 2. C^{-2}–V characteristics for the Al/SiO$_2$/n-Si Schottky Diode at 500 kHz before and afterγ-ray radiation.

$$c_2 = -\frac{2}{q\varepsilon_s N_A[\mathrm{d}(C^{-2})/\mathrm{d}V]} \cong \frac{N_A}{N'_A} = \frac{\varepsilon_i}{\varepsilon_i + q\delta N_{ss}}, \qquad (5)$$

where the oxide layer thickness, δ, is 36 Å, the dielectric constant of interfacial oxide layer is $\varepsilon_i = 3.8\varepsilon_0$ for SiO$_2$ and the value of c_2 is taken from Table 1. Also, the calculated values of V_o, V_D, N_A, W_D, E_F, $\Delta\Phi_B$, Φ_B, c_2 and N_{ss} obtained from C^{-2} to V plot at different radiation dose ranges, are presented in Table 1.

In Fig. 2, it is clear that the intercept of the C^{-2} versus V characteristics changes with increasing total dose, shifting slightly to more negative voltages. These radiation dependent experimental C–V measurements revealed that, in the γ-irradiated diodes, the barrier height Φ_B increases with increase in radiation dose [5,11,26] The increase in barrier height, Φ_B, obtained from the experimental C^{-2}–V plots, is due to an increase in V_o shown in Fig. 2. As shown in Table 1, before and after exposure of 25 kGy dose, the C–V measurements revealed that the values of barrier height (Φ_B) changes from 0.761 to 0.965 eV and the acceptor concentration from 1.19×10^{15} to 7.2×10^{14} cm^{-3}. In C–V measurements, only the edge of depletion layer is

Table 1
Electrical parameters of Al/SiO$_2$/n-Si (MIS) structures obtained from C^{-2}–V plot before and after radiation between 0 and 25 kGy

Radiation (kGy)	V_0 (V)	V_D (eV)	N_A ($\times 10^{15}$ cm^{-3})	E_F (eV)	W_D ($\times 10^{-5}$ cm)	$\Delta\Phi_B$ (meV)	Φ_B (eV)	c_2	N_{ss} (eV^{-1} cm^{-2})
Before irradiation	0.494	0.520	1.19	0.256	4.421	14.212	0.761	0.344	7.721×10^{12}
1	0.507	0.532	1.08	0.259	4.474	13.864	0.776	0.311	8.947×10^{12}
5	0.630	0.656	0.87	0.264	4.967	13.162	0.906	0.253	1.195×10^{13}
25	0.683	0.709	0.72	0.269	5.163	12.509	0.965	0.206	1.556×10^{13}

modulated and short-wavelength potential fluctuations at the oxide–semiconductor interface are screened at the edge of the space–charge region [14,27–33]. The capacitance (C) is insensitive to potential fluctuations at a length scale of less than the space–charge width. In addition, the C–V technique measures the barrier height of MIS structure taking averages over the whole area. As shown in Table 1, the obtained values of the mean density of interface states (N_{ss}) between oxide and semiconductor (SiO_2/Si) interface increase with increasing radiation dose. This result is assumed to be due to the traps created by irradiation in oxide layer.

The conductance technique [13,14,24,25] is based on the conductance losses resulting from the exchange of majority carriers between the interface states and majority carrier band of the semiconductor when a small ac signal is applied to the MIS or MOS structures. The applied ac signal causes the Fermi level to oscillate about the mean positions governed by the dc bias, when the MOS structure is in the depletion. Fig. 3 shows the measured conductance–voltage (G/ω–V) characteristics of the studied sample at various radiation γ-doses between 0 and 25 kGy.

The values of conductance decrease with increasing radiation dose. This behavior is attributed to the production of the lattice defects in the form of vacancies, defect clusters and dislocation loops near the SiO_2/Si interface due to the increase of the irradiation.

There are several methods to extract the series resistance of MIS and MOS structures in literature [34,35]. In this study we have used the conductance method developed by Nicollian and Goetzberger [33,36]. The real series resistance of these structures can be subtracted from the measured capacitance (C_m) and conductance (G_m) in strong accumulation region at high frequency ($f \geqslant 500$ kHz) [21,33,36]. In addition, the voltage and frequency dependence of the series resistance profile can be obtained from the C–V and G/ω–V curves.

The measured admittance (Y_m) at strong accumulation of MIS or MOS structures using the parallel RC circuit [13,14,24] is equivalent to the total circuit admittance as

$$Y_m = G_m + j\omega C_m. \tag{6}$$

Comparing the real and imaginary part of the admittance, the series resistance is given by [14,35,36]

$$R_s = \frac{G_m}{G_m^2 + (\omega C_m)^2}, \tag{7}$$

where C_m and G_m represent the measured capacitance and conductance in strong accumulation region, respectively and ω is the angular frequency. The series resistance is an important parameter to determine the noise ratio of device in terms of radiation dose. The values of R_s were calculated from Eq. (7) according to [33] and are given in Fig. 4. The values of R_s increase with increasing dose rate. However, the exposure of studied sample to the $^{60}C_o$ (γ-ray) irradiation were not chance the relation between voltage and R_s. The use of Eq. (7) produces a series resistance dependence on voltage. As seen in Fig. 4, in the inversion region, the value of the series resistance increases with increasing voltage and in the depletion regions, about −2 to 0 V, gives a peak [11,26,37]. This voltage dependence of R_s is the result of voltage-dependent charges such as interface charge, fixed oxide charge, oxide-trapped charge and mobile oxide charge.

The obtained R_s values are used to correct the measured C–V and G/ω–V curves. As it can be seen in Figs. 1 and 3, the measured capacitance and conductance are dependent

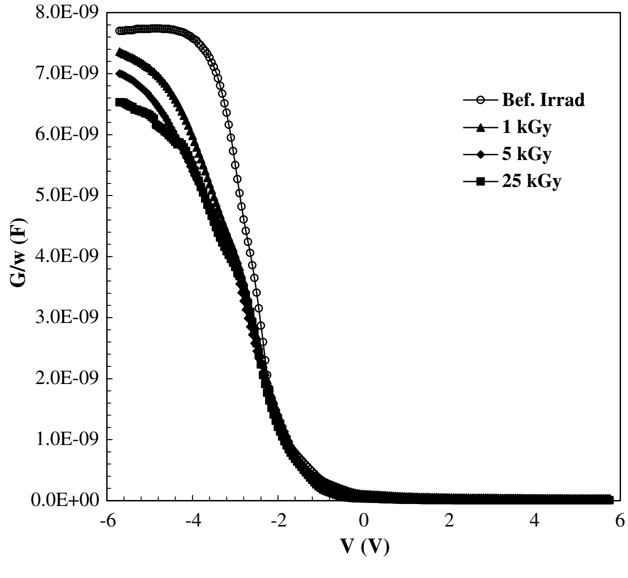

Fig. 3. The G/ω–V characteristics of the Al/SiO_2/p-Si Schottky diode before and after γ-ray irradiation obtained at 500 kHz and room temperature.

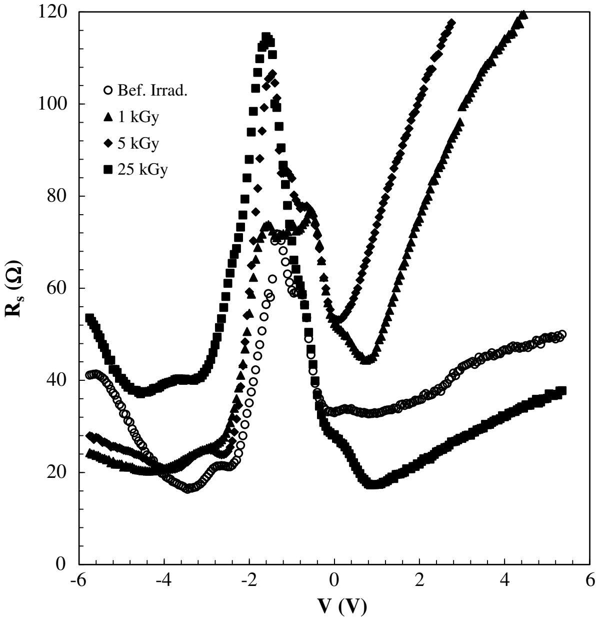

Fig. 4. Series resistance (R_s) versus gate bias under different irradiation doses at 500 kHz and room temperature.

on radiation dose especially at reverse bias. In order to obtain the real diode capacitance C_c and conductance G_c/ω, the capacitance and conductance at 500 kHz measured under forward and reverse bias were corrected for removing the effect of series resistance using following equations. The corrected capacitance C_c and conductance G_c are calculated from the relations [14]

$$C_c = \frac{\left[G_m^2 + (\omega C_m)^2\right] C_m}{a^2 + (\omega C_m)^2} \tag{8}$$

and

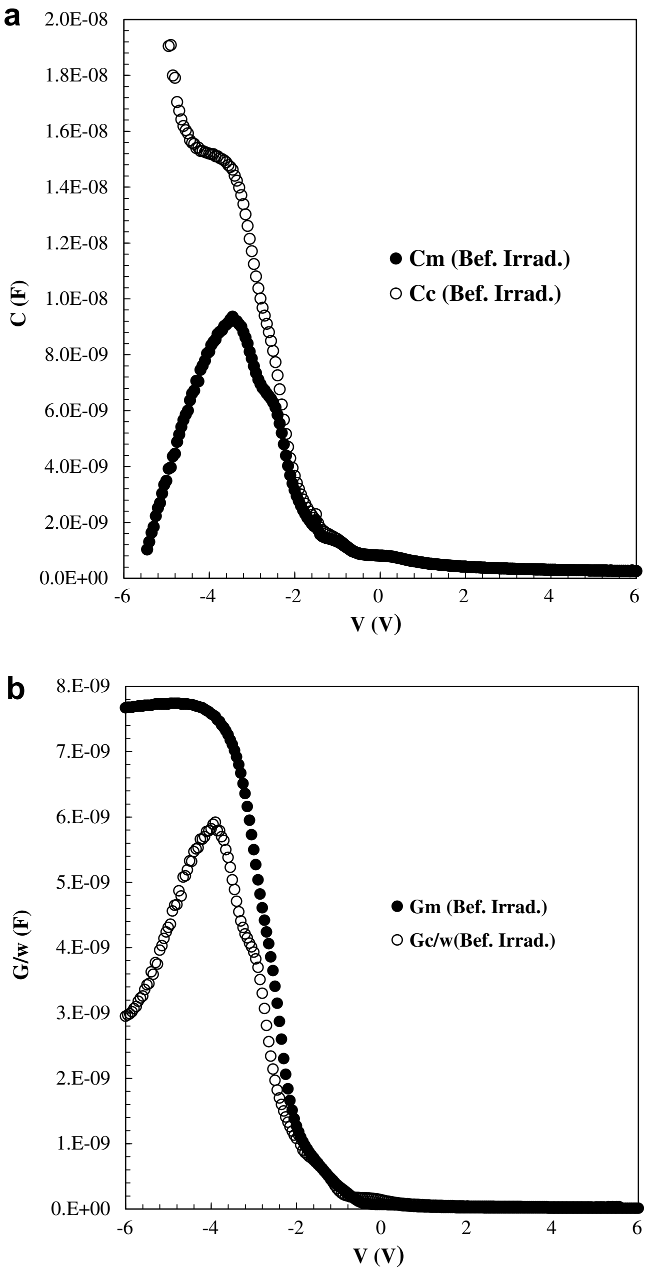

Fig. 5. The voltage-dependent plots of the corrected (a) capacitance and (b) conductance curves before irradiation at 500 kHz and room temperature.

$$G_c = \frac{G_m^2 + (\omega C_m)^2 a}{a^2 + (\omega C_m)^2}, \tag{9}$$

where

$$a = G_m - \left[G_m^2 + (\omega C_m)^2\right] R_s, \tag{10}$$

where C_m and G_m are the measured capacitance and conductance, respectively.

When the correction is made on the *C–V* and G/ω curves, the values of the corrected capacitance C_c and conductance G_c/ω before irradiation change under forward and reverse biases are seen in Fig. 5(a) and (b) respectively. As seen in these figures, while the values of corrected capacitance are greater than the measured values of capacitance the values of corrected conductance are smaller than the measured values because of elimination of the series resistance effect [38]. Similar curves are obtained after-irradiation

4. Conclusion

To investigate the radiation effects on the electrical characteristics of Al/SiO$_2$/n-Si (MIS) structures using *C–V* and G/ω–*V* measurements, the diode was exposed to a γ-radiation source at dose rate of 2.12 kGy/s. The obtained experimental results show a decrease in capacitance and conductance after γ-irradiation, implying a widening in the semiconductor depletion width due to the irradiation-induced defects at the SiO$_2$/p-Si interface. Exposure to increasing cumulative γ-ray doses was found to have the following effects: (a) a manifested increases in the barrier height obtained from the reverse bias *C–V* measurements, (b) increases in the series resistance R_s obtained from *C–V* and G/ω–*V* measurements in the reverse bias region and (c) increase in the interface states N_{ss} with increasing radiation dose. As a result, the capacitance and conductance of the γ-irradiated Al/SiO$_2$/n-Si (MIS) structures manifest that there is an increase in the interface states and depletion larger width. In addition, both the high frequency *C* and *G* are found to be strongly affected by series resistance of the device.

References

[1] T.P. Ma, P.V. Dressendorfer, Ionizing Radiation Effect in MOS Devices and Circuits, Wiley, New York, 1989.
[2] T.R. Oldham, Ionizing Radiation Effects in MOS Oxides, World Scientific Publishing, Singapore, 1999.
[3] S. Kaschieva, Zh. Todorova, S.N. Dmitriev, Vacuum 76 (2004) 307.
[4] E.A. De Vascancelas, E.F. Da Silva Jr., H. Khoury, V.N. Freire, Semicond. Sci. Technol. 15 (2000) 794.
[5] G.A. Umana-Membreno, J.M. Dell, G. Parish, B.D. Nener, L. Faraone, U.K. Mishra, IEEE Trans. Electron. Dev. 50 (2003) 2326.
[6] R.K. Chauhan, P. Chakrabarti, Microelectron. J. 33 (2002) 197.
[7] K. Naruke, M. Yoshida, K. Maegushi, H. Tango, IEEE Trans. Nucl. Sci. NS-30 (6) (1983) 4054.
[8] P.S. Winokur, J.M. McGarrity, H.E. Boesch, IEEE Trans. Nucl. Sci. 23 (1976) 1580.
[9] P.S. Winokur, J.R. Schwank, P.J. McWhorter, P.V. Dressendorfer, D.C. Turpin, IEEE Trans. Nucl. Sci. 31 (6) (1984) 1453.

[10] T.P. Ma, Semicond. Sci. Technol. 4 (1989) 1061.

[11] M.Y. Feteha, M. Soliman, N.G. Gomaa, M. Ashry, Renew. Energ. 26 (2002) 113.

[12] A. Tataroğlu, Ş. Altındal, S. Karadeniz, N. Tuğluoğlu, Microelectron. J. 34 (2003) 1043.

[13] E.H. Nicollian, J.R. Brews, MOS Physics and Technology, John Wiley & Sons, New York, 1982.

[14] S.M. Sze, Physics of Semiconductor Devices, second ed., John Wiley & Sons, New York, 1981.

[15] E.H. Rhoderick, R.H. Williams, Metal–Semiconductor Contacts, second ed., Clarendon Press, Oxford, 1978.

[16] C. Sah, Fundamental of Solid-State Electronics, World Scientific Publishing, Singapore, 1991.

[17] Ş. Karataş, A. Türüt, Ş. Altındal, Nucl. Instr. and Meth. A 555 (2005) 260.

[18] A. Kinoshita, M. Iwami, K. Kobayashi, I. Nakano, R. Tanaka, T. Kamiya, A. Ohi, T. Ohshima, Y. Fukushima, Nucl. Instr. and Meth. A 541 (2005) 213.

[19] E.A. De Vascancelas, E.F. Da Silva Jr., Semicond. Sci. Technol. 12 (1997) 1032.

[20] B. Akkal, Z. Benamara, B. Gruzza, L. Bideux, Vacuum 57 (2000) 219.

[21] K. Hung, Y.C. Cheng, J. Appl. Phys. 62 (1987) 4204.

[22] S. Özdemir, Ş. Altındal, Sol. Energ. Mater. Sol. Cell 32 (1994) 115.

[23] S.J. Fonash, J. Appl. Phys. 54 (4) (1983) 1966.

[24] P. Chattopadhyay, A.N. Daw, Solid State Electron. 29 (1986) 555.

[25] A. Singh, Solid State Electron. 28 (1985) 223.

[26] A.P. Karmarkar, B.D. White, D. Buttari, D.M. Fleetwood, R.D. Schrimpf, R.A. Weller, L.J. Brillson, U.K. Mishra, IEEE Trans. Nucl. Sci. 52 (6) (2005) 2239.

[27] P. Cova, A. Singh, Solid State Electron. 33 (1) (1990) 11.

[28] J.W. Stacey, R.D. Schrimpf, D.M. Feetwood, K.C. Holmes, IEEE Trans. Nucl. Sci. 51 (6) (2004) 3686.

[29] S.N. Rashkeev, C.R. Cirba, D.M. Fleetwood, R.D. Schrimpf, S.C. Witczak, A. Michez, S.T. Pantelides, IEEE Trans. Nucl. Sci. 49 (6) (2002) 2650.

[30] R.T. Tung, Mater. Sci. Eng. R 35 (2001) 1.

[31] S. Chand, J. Kumar, J. Appl. Phys. A 63 (1996) 171.

[32] W.M.R. Divigalpitiya, Sol. Energ. Mater. 18 (1989) 253.

[33] E.H. Nicollian, A. Goetzberger, Appl. Phys. Lett. 7 (1965) 216.

[34] K. Sato, Y. Yasamura, J. Appl. Phys. 58 (1985) 3656.

[35] H. Norde, J. Appl. Phys. 50 (1979) 5052.

[36] E.H. Nicollian, A. Goetzberger, Bell Syst. Tech. J. 46 (1967) 1055.

[37] P. Jayavel, J. Kumar, K. Santhakumar, P. Magudapathy, K.G.M. Nair, Vacuum 57 (2000) 51.

[38] İ. Dökme, Ş. Altındal, J. Phys. B: Condens. Matter 391 (2007) 59.